Published in final edited form as:

Circulation. 2020 January 21; 141(3): 217–233. doi:10.1161/CIRCULATIONAHA.119.042178.

A Novel Role of Cyclic Nucleotide Phosphodiesterase 10A in Pathological Cardiac Remodeling and Dysfunction

Si Chen, MS[1,2], **Yishuai Zhang, PhD**[1], **Janet K. Lighthouse, PhD**[1], **Deanne M. Mickelsen, BS**[1], **Jiangbin Wu, PhD**[1], **Peng Yao, PhD**[1,3], **Eric M. Small, PhD**[1], **Chen Yan, PhD**[1,*]

[1]Aab Cardiovascular Research Institute, Department of Medicine, University of Rochester School of Medicine and Dentistry, Rochester, NY, USA.

[2]Department of Pharmacology and Physiology, University of Rochester School of Medicine and Dentistry, Rochester, NY, USA.

[3]Department of Biochemistry and Biophysics, University of Rochester School of Medicine and Dentistry, Rochester, NY, USA.

Abstract

Background——Heart failure is a leading cause of death worldwide. Cyclic nucleotide phosphodiesterases (PDEs), through degradation of cyclic nucleotides, play critical roles in cardiovascular biology and disease. Our preliminary screening studies have revealed PDE10A upregulation in the diseased heart. However, the role of PDE10A in cardiovascular biology and disease are largely uncharacterized. The current study is aimed to investigate the regulation and function of PDE10A in cardiac cells and in the progression of cardiac remodeling and dysfunction.

Methods——We used isolated adult mouse cardiac myocytes (CMs) and fibroblasts (CFs), as well as preclinical mouse models of hypertrophy and/or heart failure. The PDE10A selective inhibitor TP-10, and global PDE10A knock out mice (PDE10A-KO) were used.

Results——We found that PDE10A expression remains relatively low in normal and exercised heart tissues. However, PDE10A is significantly upregulated in mouse and human failing hearts. *In vitro*, PDE10A deficiency or inhibiting PDE10A with selective inhibitor TP-10, attenuated CM pathological hypertrophy induced by Angiotensin II (Ang II), phenylephrine (PE), and isoproterenol (ISO), but did not affect CM physiological hypertrophy induced by insulin-like growth factor 1 (IGF-1). TP-10 also reduced transforming growth factor-β (TGF-β)-stimulated CF activation, proliferation, migration and ECM synthesis. TP-10 treatment elevated both cAMP and cGMP levels in CM and CF, consistent with PDE10A as a cAMP/cGMP dual-specific PDE. *In vivo*, global PDE10A deficiency significantly attenuated myocardial hypertrophy, cardiac fibrosis, and/or dysfunction induced by chronic pressure overload via thoracic aorta constriction (TAC) or chronic neurohormonal stimulation via Ang II infusion. Importantly, we demonstrated that the pharmacological effect of TP-10 is specifically through PDE10A inhibition. In addition, TP-10 is able to reverse pre-established cardiac hypertrophy and dysfunction. RNA-Sequencing and

*Corresponding author: Chen Yan, PhD, Aab Cardiovascular Research Institute, University of Rochester School of Medicine and Dentistry, Rochester, NY, USA, 14642; Phone: 585-276-7704; Fax: 585-276-5830; chen_yan@urmc.rochester.edu.

Disclosure

None

bioinformatics analysis further identified a PDE10A-regualted transcriptome involved in cardiac hypertrophy, fibrosis, and cardiomyopathy.

Conclusions——Taken together, our study elucidates a novel role for PDE10A in the regulation of pathological cardiac remodeling and development of heart failure. Given that PDE10A has been proven to be a safe drug target, PDE10A inhibition may represent a novel therapeutic strategy for preventing and treating cardiac diseases associated with cardiac remodeling.

Keywords

cardiac hypertrophy; cardiac remodeling; cyclic nucleotide phosphodiesterases

Introduction

Heart failure (HF), a leading global cause of morbidity and mortality, is a condition that heart is unable to pump sufficient blood to the body[1, 2]. HF is characterized by pathological hypertrophy, cell death, fibrosis, chamber dilation, and contractile dysfunction[1]. In response to pathological stimuli such as hypertension, neurohumonal overactivation, myocardial injury, or genetic mutation, the heart can undergo pathological remodeling by increasing cardiac myocyte (CM) size and CM loss, leading to contractile dysfunction[3]. In addition, chronic stress triggers cardiac fibroblasts (CFs) to transdifferentiate into highly proliferative and migratory myofibroblasts, leading to excess production of extracellular matrix (ECM) and fibrosis, a hallmark of pathological remodeling[4]. These pathological processes eventually lead to reduced cardiac tissue compliance and the development of end-stage HF. Therefore, identifying novel molecular targets involved in pathological cardiac remodeling and dysfunction continues to be of great interest.

Cyclic nucleotide signaling regulates numerous biological functions and pathological processes in the cardiovascular system, ranging from short-term muscle contraction/relaxation to long-term cell growth/survival and structural remodeling[5, 6]. Phosphodiesterases (PDEs), by degradation of cyclic nucleotides, play important roles in the regulation of intracellular cyclic nucleotide levels, duration of signal, and compartmentalization[7, 8]. Disruption in cyclic nucleotide homeostasis due to alterations in PDE expression and/or activity results in the progression of various diseases[7]. The PDE superfamily is comprised of 11 structurally related but functionally distinct gene families from PDE1 to PDE11, with differences in their molecular structures, catalytic properties, mechanisms of regulation, tissue distribution, and cellular functions[9]. Up to now, at least 7 PDE family members have been described in the heart: PDE1, 2, 3, 4, 5, 8, and 9[7]. Each regulates distinct cyclic nucleotide signaling pathways and plays different roles in cardiac diseases.

PDE10A was first identified as a dual cAMP-cGMP PDE[10–12]. Its high expression in medium spiny neurons of the human striatum led to the development of several PDE10A inhibitors with the intent to treat various psychiatric/neurodegenerative disorders, including schizophrenia[13, 14] and Huntington's disease[15, 16]. Importantly, several PDE10A inhibitors have been tested in humans and successfully passed phase I clinical trials (ClinicalTrials.gov), indicating PDE10A can be a safe "druggable" target. To date, studies of

PDE10A outside the central nervous system have been limited. The role of PDE10A in the cardiovascular system remains uncharacterized. In this study, we discovered abnormal induction of PDE10A expression in failing hearts. We determined the pathological effects of PDE10A activation in CMs and CFs. We demonstrated the protective effects of PDE10A inactivation against pathological cardiac remodeling and/or progression to HF in different preclinical mouse cardiac disease models. Thus, PDE10A inhibition may represent a novel therapeutic strategy in preventing and treating cardiac diseases associated with cardiac remodeling. Additionally, understanding the role of PDE10A in cardiac biology and disease is essential when using PDE10A inhibitors to treat other disorders.

Methods

All data, analytic methods, and study materials will be made available to other researchers for purposes of reproducing results or replicating the procedures. Detailed methods are provided in the online-only Data Supplement.

Animal models

All animal procedures were performed in accordance with the National Institutes of Health (NIH) and University of Rochester institutional guidelines. For experiments with genetically modified mice, age/sex/genetic background matched mice were randomly separated into indicated groups. For the Angiotensin II (Ang II) infusion model, PDE10A-wild type (PDE10A-WT) and PDE10A-knockout (PDE10A-KO) mice from sibling mating at 8–12 weeks of age were subjected to subcutaneous infusion with vehicle saline or Ang II (1.4 mg/kg/day) for 14 days using osmotic mini-pumps. For the transverse aorta constriction (TAC) model, PDE10A-WT and PDE10A-KO male or female mice aged 8–12 weeks were randomly separated into indicated groups. M-Mode echocardiography was performed on short axis in anesthetized mice to assess ventricular function. The TAC surgery and echocardiogram were performed by microsurgeons in a blind manner. For chronic treadmill training, mice aged 12–14 weeks were subjected to a motorized treadmill every day for 28 days[17]. The swim model was performed as previously described[17], where mice aged 12–14 weeks were conditioned to exercise by increasing the time spent swimming each day.

Adult mouse CM and CF isolation and culture

Adult mouse CMs and CFs were isolated by enzymatic dissociation using collagenase type II (Worthington) in a Langendorff perfusion system as previously described[18–20]. CMs were cultured in the presence of blebbistatin (a myosin II inhibitor) to block myocyte contraction and to extend their survival during the culture as described[18, 20, 21]. Adult mouse CM hypertrophy was induced by indicated stimuli for 72 h. CFs were isolated along with CMs by centrifuging the supernatant remaining after the initial setting phase of CM and were cultured as described[18]. CFs without passaging were used for experiments.

Statistics

All data are presented as mean ± SEM. GraphPad Prism 7.0 was used for statistical analysis. Comparisons between two groups were performed using unpaired Student’s t-test. One-way, two-way or repeated measures ANOVA followed by Holm-Sidak post-hoc test was used to

determine the statistical significance among groups. A P-value < 0.05 was considered statistically significant.

Results

PDE10A expression is upregulated in human and mouse failing hearts, as well as in isolated adult mouse CMs and CFs stimulated with pro-hypertrophic and pro-fibrotic stimulus, respectively.

Our preliminary screening studies for dysregulated PDE expression in mouse hearts revealed PDE10A upregulation in the diseased hearts. To validate this observation, we assessed PDE10A mRNA and protein levels using different approaches in both mouse and human failing hearts. There are three major PDE10A variants described to date[22] and PDE10A2 is the major PDE10A isoform expressed in the heart (Supplemental Figure S1A–B). We found an upregulation of PDE10A2 mRNA (refer to as PDE10A mRNA) and protein levels in mouse failing hearts induced by TAC compared to control sham hearts (Figure 1A–B). Consistently, PDE10A cAMP-hydrolyzing activity was significantly increased in mouse failing hearts (Figure 1C). PDE10A protein levels in mouse failing hearts were also predominantly induced in CMs and activated CFs (Figure 1D and Supplemental Figure S2A). The specificity of PDE10A staining was verified by immunoglobin G (IgG) control or in PDE10A-KO heart tissues (Supplemental Figure S2B–E). In primary cultured adult mouse CMs, Ang II significantly increased PDE10A mRNA levels (Figure 1E) and protein expression (Figure 1F). Transforming growth factor-β (TGF-β) elevated PDE10A mRNA levels (Figure 1G) and protein expression (Figure 1H) in CFs. Immunostaining of endogenous PDE10A or PDE10A2 overexpression exhibited unique expression and localization of PDE10A to the plasma membrane (Supplemental Figure S2F–G). Consistent with these findings, we showed that the PDE10A mRNA levels (Figure 2A) and protein expression (Figure 2B) were significantly elevated in human failing hearts compared with non-failing controls. An increase of PDE10A cAMP-hydrolyzing activity was also found in human failing hearts (Figure 2C). Immunostaining of PDE10A further revealed that PDE10A expression was low in non-failing human hearts but largely induced in CMs and activated CFs of failing hearts (Figure 2D).

The heart can enlarge in size with preserved function in response to exercise, referred to as physiological hypertrophy[23]. To assess the regulation of PDE10A in physiological hypertrophy, we examined the expression of PDE10A in heart samples from mice subjected to either treadmill running or swimming exercise[17]. In contrast to pathological hypertrophy, we observed a downregulation of PDE10A in response to exercise training at the mRNA level (Supplemental Figure S3A–B). These data suggest that PDE10A expression is differentially regulated in pathological versus physiological hypertrophy.

PDE10A inhibition increases both cAMP and cGMP levels in CMs and CFs.

PDE10A is able to hydrolyze both cAMP and cGMP[10–12]. PDE10A inhibitor treatment increased both cAMP and cGMP levels in rodent brains[24]. We therefore examined the effects of PDE10A selective inhibitor TP-10 (Supplemental Figure S4A) on cAMP and cGMP levels in CMs and CFs. We found that TP-10 treatment significantly increased both

cAMP (Supplemental Figure S4B) and cGMP (Supplemental Figure S4C) levels in CM. Similarly, TP-10 also significantly elevated cAMP (Supplemental Figure S4D) and cGMP (Supplemental Figure S4E) in CFs. These results suggest that PDE10A regulates cAMP- and cGMP-dependent functions in CMs and CFs.

PDE10A inhibition and deficiency attenuate CM pathological hypertrophy *in vitro*.

Pathological CM hypertrophy is one of the hallmarks of pathological remodeling. Since PDE10A expression is upregulated in CMs of failing hearts (Figure 1D and 2D) and in cultured CMs treated with pro-hypertrophic stimuli (Figure 1E–F), we examined the effects of PDE10A inhibition or deficiency on CM hypertrophy by stimulating cultured adult mouse CMs with different pathological hypertrophic stimuli such as Ang II, isoproterenol (ISO), and/or phenylephrine (PE) for 3 days with a successful preservation of sarcomeric/tubular structure (Supplemental Figure S5A). CM hypertrophy was evaluated using several methods including myocyte cell surface area (CSA), width/length measurements, protein synthesis, and hypertrophic marker expression. We found that Ang II-stimulated CM hypertrophy, as indicated by increases in CM CSA, length and width, were largely inhibited by TP-10 (Figure 3A–D). Additionally, Ang II-induced protein synthesis, assessed by [^{3}H]-leucine incorporation (Figure 3E) and hypertrophic marker β-myosin heavy chain (β-MHC) expression (Figure 3F), were also inhibited by TP-10. TP-10 attenuated Ang II-induced CM hypertrophy in a dose-dependent manner (Supplemental Figure S5B). In addition, ISO- and PE-induced hypertrophy was partially attenuated by TP-10 (Supplemental Figure S5C–D). TP-10 inhibits PDE10A activity at IC_{50} 0.3nM in test tubes, with at least 2500-fold selectivity for PDE10A over other PDEs[24–26]. However, TP-10 is highly protein bound once introduced in the culture medium, and thus higher doses of TP-10 are often needed[25, 27]. To confirm the specificity of TP-10, we showed that TP-10 (at doses ≤ 5 μM) displayed no additional effect on ISO-stimulated CM hypertrophy in KO CMs (Figure S5E). To further confirm the role of PDE10A, we overexpressed PDE10A2 with C-terminal fused GFP in WT CMs. Interestingly, PDE10A2-GFP expression sensitized WT CMs to Ang II-stimulated myocyte hypertrophy, which was completely abolished by TP-10 (Figure 3G). PDE10A2-GFP expression was verified by Western blotting and PDE10A activity (Supplemental Figure S5F–G).

We next examined the effects of PDE10A deficiency on CM hypertrophy. The CSA of CMs isolated from PDE10A-WT and PDE10A-KO mice were similar at the unstimulated basal state (Supplemental Figure S6A). In contrast to WT CMs, Ang II failed to stimulate CM hypertrophy in PDE10A-KO CMs as assessed by CM CSA (Figure 3H), width (Figure 3I), and length measurements (Figure 3J), as well as [^{3}H]-leucine incorporation (Figure 3K) and β-MHC expression (Figure 3L). Similar to the effect of TP-10 in WT CM, ISO-induced hypertrophy was partially attenuated by PDE10A deficiency (Supplemental Figure S5E). We then rescued PDE10A-KO CM by ectopically expressing PDE10A2. The PDE10A2 protein and activity are roughly 2–3 times that seen in Ang II-stimulated PDE10A-WT CMs (Supplemental Figure S6B–F). We found that PDE10A expression re-sensitized KO CMs to Ang II-stimulated hypertrophy. This rescue was ameliorated by TP-10 (Figure 3M).

We next confirmed our findings using the human CM cell line AC16, a proliferating cell line derived from SV40 transformed adult human ventricular CMs[28]. Consistent with the results obtained using adult mouse CMs, we detected an increase in PDE10A levels in AC16 CMs treated with Ang II (Supplemental Figure S7A). We also found that Ang II, ISO, and PE stimulated AC16 hypertrophy, which was abolished by TP-10 (Supplemental Figure S7B–E).

In contrast to the pathological hypertrophy induced by Ang II, ISO, and/or PE, insulin-like growth factor 1 (IGF-1) has been implicated in the induction of physiological hypertrophy[23]. We thus stimulated CMs with IGF-1 to mimic physiological hypertrophy. Interestingly, both TP-10 and PDE10A-KO failed to attenuate IGF-1 induced CM hypertrophy (Supplemental Figure S8A–B). Together these results strongly suggest that PDE10A plays a critical causative role in promoting CM pathological hypertrophy but not physiological hypertrophy.

PDE10A inhibition and deficiency attenuate CF activation, proliferation, migration and ECM synthesis.

Since PDE10A expression is upregulated in CFs stimulated with a pro-fibrotic stimulus (Figure 1G–H), we sought to determine the role of PDE10A in regulating CF functions. We first examined the effects of PDE10A inhibition/deficiency on CF activation or phenotype change to myofibroblast through assessing the induction of α-smooth muscle actin (α-SMA) and periostin (Postn), validated myofibroblast markers. We found that TP-10 significantly inhibited TGF-β-stimulated increases in α-SMA (Figure 4A) and Postn (Figure 4B) mRNA levels. TP-10 also elicited dose-dependent effects on α-SMA mRNA levels (Supplemental Figure S9A). Western blot and immunostaining further confirmed the inhibitory effects of PDE10A deficiency and/or inhibition on α-SMA protein induction by TGF-β (Supplemental Figure S9B–C). Activated CFs gain the capacity to proliferate and migrate. We found that CF proliferation and migration induced by TGF-β were blocked by TP-10 (Figure 4C–D). In addition, TP-10 blocked the induction of ECM proteins, including collagen1A (Col1a1) (Figure 4E) and fibronectin1 (Fn1) (Figure 4F), as well as blocked TGF-β induced collagen synthesis assessed by [^{3}H]-proline incorporation (Supplemental Figure S9D). Western blot further confirmed the suppression of TP-10 on Col1a protein induction by TGF-β (Supplemental Figure S9E). Similar to TP-10, PDE10A deficiency significantly diminished TGF-β induced CF activation (Figure 4G–H), proliferation (Figure 4I), migration (Figure 4J) and ECM synthesis (Figure 4K–L, and Supplemental Figure S9F) seen in PDE10A-WT CFs.

Consistent with the results obtained using adult mouse CFs, we also observed an increase in PDE10A mRNA levels in primary human CFs stimulated with TGF-β (Supplemental Figure S10A). TP-10 attenuated TGF-β-induced human CF activation (Supplemental Figure S10B–C) and ECM synthesis (Supplemental Figure S10D). Together these results support a critical role of PDE10A in promoting stress-induced CF activation, proliferation and ECM synthesis.

PDE10A deficiency attenuates stress-induced cardiac remodeling and dysfunction *in vivo*.

Given the upregulation of PDE10A expression in failing hearts and the pathological roles of PDE10A in isolated CMs and CFs, we attempted to determine the role of PDE10A in pathological cardiac remodeling and dysfunction *in vivo* using PDE10A deficient mice. Global PDE10A-KO mice on a C57BL/6J background have normal growth rates and feeding patterns, as well as normal nursing and mating behavior[29]. We also did not observe a significant alteration of other PDEs between PDE10A-WT and -KO hearts (Supplemental Figure S11). We first used the chronic pressure overload model via TAC, a well-established mouse heart failure model. Interestingly, PDE10A-KO mice exhibited a lower mortality rate compared to PDE10A-WT mice after TAC (Figure 5A). Global heart size (Figure 5B, and Supplemental Figure S12A), ratio of ventricular weight to body weight (HW/BW) (Supplemental Figure S12B), and ratio of ventricular weight to tibia length (HW/TL) (Figure 5C) all significantly increased in PDE10A-WT mice with TAC compared to sham. These changes induced by TAC were markedly attenuated in PDE10A-KO mice. Echocardiography was performed to monitor the progression of cardiac structural and functional changes (Figure 5D and Supplemental Table S1). After TAC, PDE10A-WT mice experienced a time-dependent loss of contractile function, which was significantly improved in PDE10-KO mice (Supplemental Table S1, Figure 5E, and Supplemental Figure S12C). In addition, left ventricular internal diameter (LVIDs and LVIDd) (Supplemental Table S1, and Figure 5F–G) and left ventricular mass (Supplemental Table S1, and Supplemental Figure S12D) were significantly reduced in PDE10A-KO mice.

Next, we performed histological analysis to further evaluate myocardial hypertrophy and fibrosis in heart tissues. We found that TAC induced a significant increase in cross-sectional area (CSA) in PDE10A-WT hearts, which was markedly decreased in PDE10A-KO hearts (Figure 5H–I). Picrosirius red staining showed that fibrosis was significantly reduced in PDE10A-KO hearts compared with PDE10A-WT hearts (Figure 5J–K, and Supplemental Figure S12E). These results together suggest that PDE10A deficiency plays a protective role in TAC-induced cardiac hypertrophy, fibrosis, and dysfunction. It should be noted that all of these differences between PDE10A-WT and -KO mice were only observed in male mice. At similar conditions, due to less hypertrophy and heart failure after TAC, we did not observe a significant alleviation of cardiac hypertrophy, cardiac fibrosis, and dysfunction in PDE10A-KO female mice (Supplemental Figure S13A–D).

RNA-sequencing identifies transcriptome that is regulated by PDE10A.

To characterize the transcriptional changes and identify the molecular events that give rise to the antihypertrophic and antifibrotic phenotypes of PDE10A-KO mice, we performed RNA-sequencing experiments with heart samples from both PDE10A-WT and PDE10A-KO mice with sham or TAC operation. Principle component analysis (PCA) demonstrated distinct patterns of transcriptome in four groups, including PDE10A-WT/sham, PDE10A-WT/TAC, PDE10A-KO/sham, and PDE10A-KO/TAC (Figure 6A). We found that biological replicates clustered together among all groups, while each experimental group demonstrated a distinct transcriptome profile. RNA-sequencing revealed 121 genes upregulated and 249 genes downregulated in the PDE10A-WT/TAC group compared to the PDE10A-WT/sham or PDE10A-KO/sham group, which were reversed in the PDE10A-KO/TAC group, suggesting

that the alteration of these genes is dependent on PDE10A in pathological remodeling (Figure 6B). We then compared PDE10A-KO/TAC hearts with PDE10A-WT/TAC hearts, establishing differences in gene expression versus significance (P value) to visualize changes in gene expression (Figure 6C). As expected, we observed changes in pro-hypertrophic or pro-fibrotic marker genes consistent with cardiac hypertrophy and fibrosis *in vivo*, including Myh7, Nppa, Postn, Tgfb2, Ctgf, Timp1, and Col1a1 (Figure 6C).

We compared RNA-seq of PDE10A-WT/TAC and PDE10A-WT/sham groups and performed Gene Ontology analysis to determine functional changes during heart failure post-TAC. Upregulated genes included genes involved in cell migration and muscle contraction (Supplemental Figure S14A). The most significant category was extracellular matrix organization, which is consistent with findings that disruption and excess deposition of ECM are associated with heart failure[30]. Downregulated gene categories in the PDE10A-WT/TAC group included respiratory electron transport chain and metabolic process (Supplemental Figure S14B). We further compared RNA-seq between the PDE10A-KO/TAC and PDE10A-WT/TAC groups to investigate the functional relationships between genes that are dysregulated by PDE10A after TAC. We found upregulated genes were involved in translation and cellular response to unfolded proteins (Supplemental Figure S14C). Downregulated genes were involved in cytokine production, angiogenesis, and apoptotic process (Supplemental Figure S14D), which are known changes in heart failure[31–33]. We also performed Kyoto Encyclopedia of Genes and Genomes (KEGG) pathway analysis, which further revealed that PDE10A may regulate pathways pertinent to metabolic pathways, biosynthesis of amino acids, Hippo signaling, HIF-1 signaling, cardiac muscle contraction, and hypertrophic and dilated cardiomyopathy (Figure 6D–E). Furthermore, represented genes that are associated with these signaling pathways were validated by qPCR (Figure 6F). Taken together, the RNAseq results support the role of PDE10A in regulating a transcriptional profile that is consistent with its role in pathological cardiac remodeling and dysfunction.

Pharmacological effects and specificity of TP-10 on preventing stress-induced adverse cardiac remodeling.

To examine the pharmacological effects of TP-10 on pathological cardiac remodeling as well as to test the specificity of TP-10 *in vivo*, we administrated TP-10 or vehicle to both PDE10A-WT and PDE10A-KO mice subjected to chronic neurohormonal stimulation via Ang II infusion. We pretreated animals with vehicle or TP-10 (3.2 mg/kg/day) subcutaneously 2 days before initiating the vehicle- or Ang II-infusion, and continued for 2 weeks (Figure 7A). This dose of TP-10 has established efficacy in mice in previously published studies from Pfizer and does not have detectable toxicity[24]. We found that Ang II-infusion significantly induced cardiac hypertrophy in PDE10A-WT mice, as evidenced by an increase in the ratio of HW/BW (Figure 7B) as well as increased expression of hypertrophic markers ANP (Figure 7C) and β-MHC (Figure 7D). The pro-hypertrophic effects of Ang II were prevented by TP-10 treatment or in PDE10A-KO mice (Figure 7B–D). Importantly, TP-10 had no further effect on PDE10A-KO mice, suggesting the anti-hypertrophic effect of TP-10 is through PDE10A inhibition. Consistently, histological analysis showed that myocardial hypertrophy (the elevation of CSA) was significantly

induced by Ang II infusion (Figure 7E–F). TP-10 attenuated myocyte hypertrophy in PDE10A-WT hearts, yet failed to exert additional effects on PDE10A-KO hearts. Moreover, Ang II-induced cardiac fibrosis was also significantly reduced by TP-10 or PDE10A deficiency, but TP-10 had no additional effects above PDE10A deficiency (Figure 7G–H and Supplemental Figure S15A). We observed similar effects of TP-10 or PDE10A deficiency on ECM protein mRNA expression such as Col1a1 (Figure 7I) and Fn1 (Supplemental Figure S15B). Ang II induced a significant and similar upregulation of blood pressure in both PDE10A-WT and -KO mice while TP-10 did not alter blood pressure (Supplemental Figure S16A), and no changes in heart rate were observed (Supplemental Figure S16B), suggesting that PDE10A does not regulate blood pressure. These observations indicate that TP-10 attenuates Ang II-induced cardiac hypertrophy and fibrosis by specifically inhibiting PDE10A.

TP-10 intervenes the progression of pre-stimulated cardiac remodeling and dysfunction.

From the clinical aspect, it would be interesting to evaluate the effects of PDE10A inhibition with TP-10 on pre-established cardiac hypertrophy and dysfunction. To address this question, PDE10A-WT mice were first subjected to sham or TAC operation for 2 weeks, when cardiac dysfunction was already clearly evident. These mice were then randomized to receive either TP-10 (3.2mg/kg/day) or vehicle treatment 2 weeks after sham or TAC and the drug treatment was continued for 6 weeks (Figure 8A). Interestingly, we observed a progressive worsening of multiple hallmark features of cardiac hypertrophy and dysfunction, including global heart size (Figure 8B, and Supplemental Figure S17A), HW/BW (Supplemental Figure S17B), and HW/TL (Figure 8C), while TP-10 blocked the progression of cardiac remodeling. Echocardiography was performed periodically to monitor the progression of structural and functional changes (Figure 8D and Supplemental Table S2). The decreases of cardiac function in vehicle treated mice as indicated by fraction shortening (Supplemental Table S2, and Figure 8E) and ejection fraction (Supplemental Table S2, and Supplemental Figure S17C) were all alleviated by TP-10 treatment. Moreover, TP-10 treatment suppressed left ventricular mass (Supplemental Table S2, and Supplemental Figure S17D), CM hypertrophy (Figure 8F–G), induction of hypertrophic markers ANP (Figure 8H) and β-MHC (Supplemental Figure S17E), left ventricular fibrosis (Figure 8I–J, and Supplemental Figure S17F), and induction of ECM protein mRNA expression such as Col1a1 (Figure 8K). In conclusion, these results indicate that TP-10 effectively blocks the progression of adverse remodeling and dysfunction in mice with existing cardiac defects.

Discussion

In this study, we report a number of important novel findings demonstrating the role of PDE10A in the heart. To our knowledge, this is the first report of PDE10A expression and function in cardiac cells and cardiac diseases. First, by using different approaches we demonstrated that PDE10A expression and activity are significantly upregulated in mouse and human failing hearts (Figure 1 and Figure 2), but not in mice undergoing different exercise trainings (Supplemental Figure S3). In addition, we showed that PDE10A regulates CM hypertrophy in response to pathological hypertrophy stimuli (Ang II, ISO, and PE) but not the physiological hypertrophy stimulus IGF-1 (Figure 3 and Supplemental Figure S5 and

S8). These findings support the high relevance of PDE10A with pathological cardiac remodeling but not exercise-induced physiological remodeling. Although both pathological and physiological cardiac remodeling are associated with increases in heart mass, only pathological remodeling is associated with cardiac fibrosis[23, 34]. In CFs, we found that PDE10A expression was upregulated by the pro-fibrotic stimulus TGF-β (Figure 1G–H), and PDE10A regulated CF activation, proliferation, migration and ECM production (Figure 4). These findings support the role of PDE10A in cardiac fibrosis and pathological cardiac remodeling that leads to impaired myocardial compliance and development of heart failure.

Using isolated adult mouse CMs or CFs, as well as various pharmacological and genetic gain-of-function or loss-of-function approaches, we demonstrated that PDE10A directly promotes the pathogenesis of CMs and CFs, two important cardiac cell types participating in pathological cardiac remodeling. With regard to pharmacological approach, we used TP-10, a potent and selective PDE10A inhibitor in our study. Because the PDE10A inhibitor TP-10 and PDE10A deficiency elicit similar effects on CMs or CFs, we believe that PDE10A enzyme activity is essential for its pathological roles in CMs and CFs. Inhibiting PDE10A activity by TP-10 increases both cAMP and cGMP in CMs and CFs (Supplemental Figure S4, B–E), which is in line with the dual specificity of PDE10A in cyclic nucleotide hydrolysis[10–12] and also similar to the observations in TP-10 treated striatum tissues[24]. In the striatum, PDE10A inhibition has been reported to promote dopamine-mediated cAMP/PKA signaling[14, 35], ERK signaling[36, 37], or nNOS/cGMP/PKG signaling[38], thus providing protection in neurodegeneration associated with disturbances in striatal function. Studies in tumor cells revealed that PDE10A inhibition induces cGMP/PKG signaling, which antagonizes β-catenin-mediated transcription, leading to cell apoptosis[39]. However, it still remains unclear how PDE10A-mediated cAMP and cGMP signaling regulates hypertrophic and fibrotic gene expression in CMs and CFs, respectively. Future studies by our group will focus on the underlying molecular mechanisms by which PDE10A regulates pathological cardiac gene expression and disease progression in CMs and CFs.

Our study using PDE10A-KO mice in various preclinical cardiac diseased models unmasked a striking role of PDE10A deficiency in the amelioration of cardiac hypertrophy, fibrosis, and/or dysfunction. By applying TP-10 in both PDE10A-WT and -KO mice, we demonstrated the therapeutic potential of PDE10A inhibition in antagonizing pathological cardiac remodeling, and also confirmed the specificity of TP-10 on targeting PDE10A *in vivo* (Figure 7). More importantly, we found that TP-10 is able to intervene the progression of remodeling and dysfunction under the setting with pre-established cardiac defects, which is more clinically relevant (Figure 8). To further support our functional observation at the molecular level, we performed RNAseq and bioinformatics analysis, which uncovered a number of PDE10A-regulated signaling pathways and cellular processes involved in cardiac hypertrophy, fibrosis, and cardiomyopathy (Figure 6). Therefore, our findings at physiological, histological, cellular, and molecular levels consistently and strongly support that PDE10A induction likely plays a causative role in the pathogenesis of cardiac remodeling and dysfunction. PDE10A inhibition may represent a novel therapeutic strategy in combating cardiac diseases associated with adverse remodeling.

We are aware that the protective effects of PDE10A deficiency or inhibition in the heart may not be exclusively contributed by CMs and CFs. It is possible that PDE10A is also expressed in other cardiac cells, including but not limited to immune cells and microvascular endothelial cells that are also important in pathological cardiac remodeling and dysfunction[40, 41]. Therefore, the expression, regulation, and function of PDE10A in these non-CM and non-CF cells deserves to be considered and further investigated. In addition, PDE10A in other tissues may modulate cardiac remodeling and function indirectly. For example, it will be interesting to determine if PDE10A in neurons also contributes to cardiac remodeling and performance. Cell-type specific PDE10A deficient mice will be needed to address the individual cellular contributions of PDE10A in the development of cardiac remodeling and dysfunction.

In addition to PDE10A, a number of other PDEs have also been suggested to be important in cardiac hypertrophy, fibrosis, and/or dysfunction. For example, PDE1A inhibition attenuates CM hypertrophy via cGMP-PKG signaling and attenuates CF activation via both cAMP-Epac and cGMP-PKG signaling[42, 43], although the role of PDE1A in pathological cardiac remodeling *in vivo* has not yet been reported. PDE1C promotes CM hypertrophy via an unknown mechanism and promotes CF activation via CM-mediated regulation of CF function[18]. PDE2 inhibition protects the heart from pathological remodeling through regulating a localized cAMP/PKA signaling pathway[44] and a nitric oxide (NO)/guanylyl cyclase (GC)/cGMP signaling pathway[45]. PDE5 inhibition attenuates cardiac hypertrophy by potentiating NO-sGC-derived cGMP[46], while PDE9 inhibition protects against cardiac hypertrophy by potentiating natriuretic peptide (NP)-pGC-derived cGMP[47]. These findings suggest that different PDEs play unique roles in CMs and CFs, likely via regulating spatially and functionally distinct cyclic nucleotide signaling. Increasing evidence has indicated that cAMP and cGMP are compartmentalized to discrete cAMP/cGMP pools that are associated with different multi-protein complexes each containing unique receptors, cyclases, PDEs, kinases, and other signaling molecules, leading to different biological functions[43, 48]. Indeed, a number of different multi-protein complexes associated with different PDEs have been reported. For instance, PDE3A and PDE4D have been shown to interact with the phospholamban-sarcoplasmic reticulum Ca^{2+} ATPase 2 signaling complex[49, 50]. PDE9 has been reported to distinctly control NPR-derived cGMP signaling[47]. PDE1C has been reported to form a complex with the transient receptor potential-canonical (TRPC) channel and $A_{2A}R$[20]. However, it remains unclear which cAMP and cGMP signaling is modulated by PDE10A in CMs and CFs.

In summary, our data strongly support the causative role of PDE10A induction in promoting cardiac hypertrophy, fibrosis, and dysfunction, which can be ameliorated via PDE10A inhibition. The therapeutic significance of our findings is further highlighted by the fact that PDE10A is a proven safe “druggable” target. Several PDE10A inhibitors have been previously tested in humans for the treatment of schizophrenia and Huntington’s disease and successfully passed phase I (safety) clinical trials as listed in ClinicalTrials.gov: NCT01244880, NCT01918202, NCT01939548, NCT00570063, NCT01829048, NCT01175135, NCT00463372, NCT01806896, NCT02370602, NCT01923025, NCT02001389. Therefore, we believe that PDE10A inhibitors may hold great therapeutic potential for cardiac diseases associated with pathological remodeling. The knowledge of

PDE10A in cardiac biology and disease will be also valuable when treating other diseases using PDE10 inhibitors.

Supplementary Material

Refer to Web version on PubMed Central for supplementary material.

Source of Funding

This work was financially supported by National Institute of Health HL134910 and HL088400 (to C.Y.), HL132899 (to P.Y.), HL144867 and HL133761 (to E.M.S.), 5T32HL066988-15 (to J.K.L.) as well as American Heart Association 17PRE33660835 (to S.C.), 15POST25550114 (to J.K.L.) and 19POST34400013 (to J.W.).

Non-standard Abbreviations and Acronyms

CM	cardiac myocyte
CF	cardiac fibroblast
HF	heart failure
ECM	extracellular matrix
PDE	phosphodiesterase
Ang II	angiotensin II
WT	wild type
KO	knockou
TAC	transverse aortic constriction
IgG	immunoglobin G
TGF-β	transforming growth factor-β
ISO	isoproterenol
PE	phenylephrine
CSA	cell surface area/cross-sectional area
β-MHC	β-myosin heavy chain
IGF-1	insulin-like growth factor 1
α-SMA	α-smooth muscle cell actin
Postn	periostin
Col1a1	collagen1A
Fn1	fibronectin1
HW	heart weight

BW	body weight
TL	tibia length
LVID	left ventricular internal diameter
PCA	principle component analysis
KEGG	Kyoto encyclopedia of genes and genomes
NO	nitric oxide
GC	guanylyl cyclase
NP	natriuretic peptide
TRPC	transient receptor potential-canonical

References

1. Frey N and Olson EN. Cardiac hypertrophy: the good, the bad, and the ugly. Annu Rev Physiol. 2003;65:45–79. [PubMed: 12524460]
2. Benjamin EJ, Virani SS, Callaway CW, Chamberlain AM, Chang AR, Cheng S, Chiuve SE, Cushman M, Delling FN, Deo R, de Ferranti SD, Ferguson JF, Fornage M, Gillespie C, Isasi CR, Jimenez MC, Jordan LC, Judd SE, Lackland D, Lichtman JH, Lisabeth L, Liu S, Longenecker CT, Lutsey PL, Mackey JS, Matchar DB, Matsushita K, Mussolino ME, Nasir K, O'Flaherty M, Palaniappan LP, Pandey A, Pandey DK, Reeves MJ, Ritchey MD, Rodriguez CJ, Roth GA, Rosamond WD, Sampson UKA, Satou GM, Shah SH, Spartano NL, Tirschwell DL, Tsao CW, Voeks JH, Willey JZ, Wilkins JT, Wu JH, Alger HM, Wong SS, Muntner P, American Heart Association Council on E, Prevention Statistics C and Stroke Statistics S. Heart Disease and Stroke Statistics-2018 Update: A Report From the American Heart Association. Circulation. 2018;137:e67–e492. [PubMed: 29386200]
3. Hill JA and Olson EN. Cardiac plasticity. N Engl J Med. 2008;358:1370–1380. [PubMed: 18367740]
4. Porter KE and Turner NA. Cardiac fibroblasts: at the heart of myocardial remodeling. Pharmacol Ther. 2009;123:255–278. [PubMed: 19460403]
5. Guellich A, Mehel H and Fischmeister R. Cyclic AMP synthesis and hydrolysis in the normal and failing heart. Pflugers Arch. 2014;466:1163–1175. [PubMed: 24756197]
6. Rainer PP and Kass DA. Old dog, new tricks: novel cardiac targets and stress regulation by protein kinase G. Cardiovasc Res. 2016;111:154–162. [PubMed: 27297890]
7. Bobin P, Belacel-Ouari M, Bedioune I, Zhang L, Leroy J, Leblais V, Fischmeister R and Vandecasteele G. Cyclic nucleotide phosphodiesterases in heart and vessels: A therapeutic perspective. Arch Cardiovasc Dis. 2016;109:431–443. [PubMed: 27184830]
8. Chen S, Knight WE and Yan C. Roles of PDE1 in Pathological Cardiac Remodeling and Dysfunction. J Cardiovasc Dev Dis 2018;5:22.
9. Maurice DH, Ke H, Ahmad F, Wang Y, Chung J and Manganiello VC. Advances in targeting cyclic nucleotide phosphodiesterases. Nat Rev Drug Discov. 2014;13:290–314. [PubMed: 24687066]
10. Fujishige K, Kotera J, Michibata H, Yuasa K, Takebayashi S, Okumura K and Omori K. Cloning and characterization of a novel human phosphodiesterase that hydrolyzes both cAMP and cGMP (PDE10A). J Biol Chem. 1999;274:18438–18445. [PubMed: 10373451]
11. Loughney K, Snyder PB, Uher L, Rosman GJ, Ferguson K and Florio VA. Isolation and characterization of PDE10A, a novel human 3', 5'-cyclic nucleotide phosphodiesterase. Gene. 1999;234:109–117. [PubMed: 10393245]

12. Soderling SH, Bayuga SJ and Beavo JA. Isolation and characterization of a dual-substrate phosphodiesterase gene family: PDE10A. Proc Natl Acad Sci U S A. 1999;96:7071–7076. [PubMed: 10359840]

13. Duinen MV, Reneerkens OA, Lambrecht L, Sambeth A, Rutten BP, Os JV, Blokland A and Prickaerts J. Treatment of Cognitive Impairment in Schizophrenia: Potential Value of Phosphodiesterase Inhibitors in Prefrontal Dysfunction. Curr Pharm Des 2015;21:3813–3828. [PubMed: 26044976]

14. Grauer SM, Pulito VL, Navarra RL, Kelly MP, Kelley C, Graf R, Langen B, Logue S, Brennan J, Jiang L, Charych E, Egerland U, Liu F, Marquis KL, Malamas M, Hage T, Comery TA and Brandon NJ. Phosphodiesterase 10A inhibitor activity in preclinical models of the positive, cognitive, and negative symptoms of schizophrenia. J Pharmacol Exp Ther. 2009;331:574–590. [PubMed: 19661377]

15. Giampa C, Laurenti D, Anzilotti S, Bernardi G, Menniti FS and Fusco FR. Inhibition of the striatal specific phosphodiesterase PDE10A ameliorates striatal and cortical pathology in R6/2 mouse model of Huntington's disease. PLoS One. 2010;5:e13417. [PubMed: 20976216]

16. Beaumont V, Zhong S, Lin H, Xu W, Bradaia A, Steidl E, Gleyzes M, Wadel K, Buisson B, Padovan-Neto FE, Chakroborty S, Ward KM, Harms JF, Beltran J, Kwan M, Ghavami A, Haggkvist J, Toth M, Halldin C, Varrone A, Schaab C, Dybowski JN, Elschenbroich S, Lehtimaki K, Heikkinen T, Park L, Rosinski J, Mrzljak L, Lavery D, West AR, Schmidt CJ, Zaleska MM and Munoz-Sanjuan I. Phosphodiesterase 10A Inhibition Improves Cortico-Basal Ganglia Function in Huntington's Disease Models. Neuron. 2016;92:1220–1237. [PubMed: 27916455]

17. Lighthouse JK, Burke RM, Velasquez LS, Dirkx RA Jr., Aiezza A 2nd, Moravec CS, Alexis JD, Rosenberg A and Small EM. Exercise promotes a cardioprotective gene program in resident cardiac fibroblasts. JCI Insight. 2019;4:e92098.

18. Knight WE, Chen S, Zhang Y, Oikawa M, Wu M, Zhou Q, Miller CL, Cai Y, Mickelsen DM, Moravec C, Small EM, Abe J and Yan C. PDE1C deficiency antagonizes pathological cardiac remodeling and dysfunction. Proc Natl Acad Sci U S A. 2016;113:E7116–E7125. [PubMed: 27791092]

19. Chen S, Wang Z, Xu B, Mi X, Sun W, Quan N, Wang L, Chen X, Liu Q, Zheng Y, Leng J and Li J. The Modulation of Cardiac Contractile Function by the Pharmacological and Toxicological Effects of Urocortin2. Toxicol Sci. 2015;148:581–593. [PubMed: 26342213]

20. Zhang Y, Knight W, Chen S, Mohan A and Yan C. Multiprotein Complex With TRPC (Transient Receptor Potential-Canonical) Channel, PDE1C (Phosphodiesterase 1C), and A2R (Adenosine A2 Receptor) Plays a Critical Role in Regulating Cardiomyocyte cAMP and Survival. Circulation. 2018;138:1988–2002. [PubMed: 29871977]

21. Kabaeva Z, Zhao M and Michele DE. Blebbistatin extends culture life of adult mouse cardiac myocytes and allows efficient and stable transgene expression. Am J Physiol Heart Circ Physiol. 2008;294:H1667–H1674. [PubMed: 18296569]

22. MacMullen CM, Vick K, Pacifico R, Fallahi-Sichani M and Davis RL. Novel, primate-specific PDE10A isoform highlights gene expression complexity in human striatum with implications on the molecular pathology of bipolar disorder. Transl Psychiatry. 2016;6:e742. [PubMed: 26905414]

23. McMullen JR and Jennings GL. Differences between pathological and physiological cardiac hypertrophy: novel therapeutic strategies to treat heart failure. Clin Exp Pharmacol Physiol. 2007;34:255–262. [PubMed: 17324134]

24. Schmidt CJ, Chapin DS, Cianfrogna J, Corman ML, Hajos M, Harms JF, Hoffman WE, Lebel LA, McCarthy SA, Nelson FR, Proulx-LaFrance C, Majchrzak MJ, Ramirez AD, Schmidt K, Seymour PA, Siuciak JA, Tingley FD 3rd, Williams RD, Verhoest PRand Menniti FS. Preclinical characterization of selective phosphodiesterase 10A inhibitors: a new therapeutic approach to the treatment of schizophrenia. J Pharmacol Exp Ther. 2008;325:681–690. [PubMed: 18287214]

25. Verhoest PR, Chapin DS, Corman M, Fonseca K, Harms JF, Hou X, Marr ES, Menniti FS, Nelson F, O'Connor R, Pandit J, Proulx-Lafrance C, Schmidt AW, Schmidt CJ, Suiciak JA and Liras S. Discovery of a novel class of phosphodiesterase 10A inhibitors and identification of clinical candidate 2-[4-(1-methyl-4-pyridin-4-yl-1H-pyrazol-3-yl)-phenoxymethyl]-quinoline (PF-2545920) for the treatment of schizophrenia. J Med Chem. 2009;52:5188–196. [PubMed: 19630403]

26. Tuttle JB and Kormos BL. The use of PDE10A and PDE9 inhibitors for treating schizophrenia *Small Molecule Therapeutics for Schizophrenia*: Springer; 2014: 255–316.
27. Megens AA, Hendrickx HM, Hens KA, Fonteyn I, Langlois X, Lenaerts I, Somers MV, de Boer P and Vanhoof G. Pharmacology of JNJ-42314415, a centrally active phosphodiesterase 10A (PDE10A) inhibitor: a comparison of PDE10A inhibitors with D2 receptor blockers as potential antipsychotic drugs. J Pharmacol Exp Ther. 2014;349:138–154. [PubMed: 24421319]
28. Davidson MM, Nesti C, Palenzuela L, Walker WF, Hernandez E, Protas L, Hirano M and Isaac ND. Novel cell lines derived from adult human ventricular cardiomyocytes. J Mol Cell Cardiol. 2005;39:133–147. [PubMed: 15913645]
29. Siuciak JA, McCarthy SA, Chapin DS, Martin AN, Harms JF and Schmidt CJ. Behavioral characterization of mice deficient in the phosphodiesterase-10A (PDE10A) enzyme on a C57/Bl6N congenic background. Neuropharmacology. 2008;54:417–427. [PubMed: 18061215]
30. Frangogiannis NG. The extracellular matrix in myocardial injury, repair, and remodeling. J Clin Invest. 2017;127:1600–1612. [PubMed: 28459429]
31. Oka T, Akazawa H, Naito AT and Komuro I. Angiogenesis and cardiac hypertrophy: maintenance of cardiac function and causative roles in heart failure. Circ Res. 2014;114:565–571. [PubMed: 24481846]
32. Mann DL. Innate immunity and the failing heart: the cytokine hypothesis revisited. Circ Res. 2015;116:1254–1268. [PubMed: 25814686]
33. Narula J, Haider N, Arbustini E and Chandrashekhar Y. Mechanisms of disease: apoptosis in heart failure--seeing hope in death. Nat Clin Pract Cardiovasc Med. 2006;3:681–688. [PubMed: 17122801]
34. Shimizu I and Minamino T. Physiological and pathological cardiac hypertrophy. J Mol Cell Cardiol. 2016;97:245–262. [PubMed: 27262674]
35. Polito M, Guiot E, Gangarossa G, Longueville S, Doulazmi M, Valjent E, Herve D, Girault JA, Paupardin-Tritsch D, Castro LR and Vincent P. Selective Effects of PDE10A Inhibitors on Striatopallidal Neurons Require Phosphatase Inhibition by DARPP-32. eNeuro. 2015;2:ENEURO.0060–15.2015.
36. Hsu YT, Liao G, Bi X, Oka T, Tamura S and Baudry M. The PDE10A inhibitor, papaverine, differentially activates ERK in male and female rat striatal slices. Neuropharmacology. 2011;61:1275–1281. [PubMed: 21816164]
37. Kleiman RJ, Kimmel LH, Bove SE, Lanz TA, Harms JF, Romegialli A, Miller KS, Willis A, des Etages S, Kuhn M and Schmidt CJ. Chronic suppression of phosphodiesterase 10A alters striatal expression of genes responsible for neurotransmitter synthesis, neurotransmission, and signaling pathways implicated in Huntington's disease. J Pharmacol Exp Ther. 2011;336:64–76. [PubMed: 20923867]
38. Padovan-Neto FE, Sammut S, Chakroborty S, Dec AM, Threlfell S, Campbell PW, Mudrakola V, Harms JF, Schmidt CJ and West AR. Facilitation of corticostriatal transmission following pharmacological inhibition of striatal phosphodiesterase 10A: role of nitric oxide-soluble guanylyl cyclase-cGMP signaling pathways. J Neurosci. 2015;35:5781–5791. [PubMed: 25855188]
39. Lee K, Lindsey AS, Li N, Gary B, Andrews J, Keeton AB and Piazza GA. beta-catenin nuclear translocation in colorectal cancer cells is suppressed by PDE10A inhibition, cGMP elevation, and activation of PKG. Oncotarget. 2016;7:5353–5365. [PubMed: 26713600]
40. Frieler RA and Mortensen RM. Immune cell and other noncardiomyocyte regulation of cardiac hypertrophy and remodeling. Circulation. 2015;131:1019–1030. [PubMed: 25779542]
41. Kamo T, Akazawa H and Komuro I. Cardiac nonmyocytes in the hub of cardiac hypertrophy. Circ Res. 2015;117:89–98. [PubMed: 26089366]
42. Miller CL, Oikawa M, Cai Y, Wojtovich AP, Nagel DJ, Xu X, Xu H, Florio V, Rybalkin SD, Beavo JA, Chen YF, Li JD, Blaxall BC, Abe J and Yan C. Role of Ca2+/calmodulin-stimulated cyclic nucleotide phosphodiesterase 1 in mediating cardiomyocyte hypertrophy. Circ Res. 2009;105:956–964. [PubMed: 19797176]
43. Miller CL, Cai Y, Oikawa M, Thomas T, Dostmann WR, Zaccolo M, Fujiwara K and Yan C. Cyclic nucleotide phosphodiesterase 1A: a key regulator of cardiac fibroblast activation and

extracellular matrix remodeling in the heart. Basic Res Cardiol. 2011;106:1023–1039. [PubMed: 22012077]

44. Zoccarato A, Surdo NC, Aronsen JM, Fields LA, Mancuso L, Dodoni G, Stangherlin A, Livie C, Jiang H, Sin YY, Gesellchen F, Terrin A, Baillie GS, Nicklin SA, Graham D, Szabo-Fresnais N, Krall J, Vandeput F, Movsesian M, Furlan L, Corsetti V, Hamilton G, Lefkimmiatis K, Sjaastad I and Zaccolo M. Cardiac Hypertrophy Is Inhibited by a Local Pool of cAMP Regulated by Phosphodiesterase 2. Circ Res. 2015;117:707–719. [PubMed: 26243800]
45. Baliga RS, Preedy MEJ, Dukinfield MS, Chu SM, Aubdool AA, Bubb KJ, Moyes AJ, Tones MA and Hobbs AJ. Phosphodiesterase 2 inhibition preferentially promotes NO/guanylyl cyclase/cGMP signaling to reverse the development of heart failure. Proc Natl Acad Sci U S A. 2018;115:E7428–E7437. [PubMed: 30012589]
46. Takimoto E, Champion HC, Li M, Belardi D, Ren S, Rodriguez ER, Bedja D, Gabrielson KL, Wang Y and Kass DA. Chronic inhibition of cyclic GMP phosphodiesterase 5A prevents and reverses cardiac hypertrophy. Nat Med. 2005;11:214–222. [PubMed: 15665834]
47. Lee DI, Zhu G, Sasaki T, Cho GS, Hamdani N, Holewinski R, Jo SH, Danner T, Zhang M, Rainer PP, Bedja D, Kirk JA, Ranek MJ, Dostmann WR, Kwon C, Margulies KB, Van Eyk JE, Paulus WJ, Takimoto E and Kass DA. Phosphodiesterase 9A controls nitric-oxide-independent cGMP and hypertrophic heart disease. Nature. 2015;519:472–476. [PubMed: 25799991]
48. Castro LR, Verde I, Cooper DM and Fischmeister R. Cyclic guanosine monophosphate compartmentation in rat cardiac myocytes. Circulation. 2006;113:2221–2228. [PubMed: 16651469]
49. Ahmad F, Shen W, Vandeput F, Szabo-Fresnais N, Krall J, Degerman E, Goetz F, Klussmann E, Movsesian M and Manganiello V. Regulation of sarcoplasmic reticulum Ca2+ ATPase 2 (SERCA2) activity by phosphodiesterase 3A (PDE3A) in human myocardium: phosphorylation-dependent interaction of PDE3A1 with SERCA2. J Biol Chem. 2015;290:6763–6776. [PubMed: 25593322]
50. Lehnart SE, Wehrens XH, Reiken SR, JS C, Vest JA, Conti M and Marks AR. Phosphodiesterase 4D Associates with the Cardiac Calcium Release Channel (Ryanodine Receptor) and Protects form Hypertrophy and Heart failure. Circulation. 2004;110:III–227.

Clinical Perspective

What is New?

- PDE10A expression is significantly induced in mouse and human failing hearts.
- PDE10A directly promotes cardiac myocyte (CM) hypertrophic growth as well as cardiac fibroblast (CF) activation, proliferation, migration and ECM production.
- PDE10A deficiency ameliorates cardiac hypertrophy, fibrosis, and/or dysfunction in different preclinical mouse cardiac disease models.
- Inhibiting PDE10A activity with TP-10 effectively antagonizes pathological cardiac remodeling.

What Are the Clinical Implications?

- PDE10A may represent a novel therapeutic target for preventing the pathogenesis of cardiac remodeling.
- The PDE10A inhibitors have been evaluated in Phase II clinical trials for treatment of schizophrenia, suggesting PDE10A is a safe “druggable” target.
- Our results with TP-10 suggest the potential therapeutic effect of targeting PDE10A on antagonizing the development of pathological cardiac remodeling.

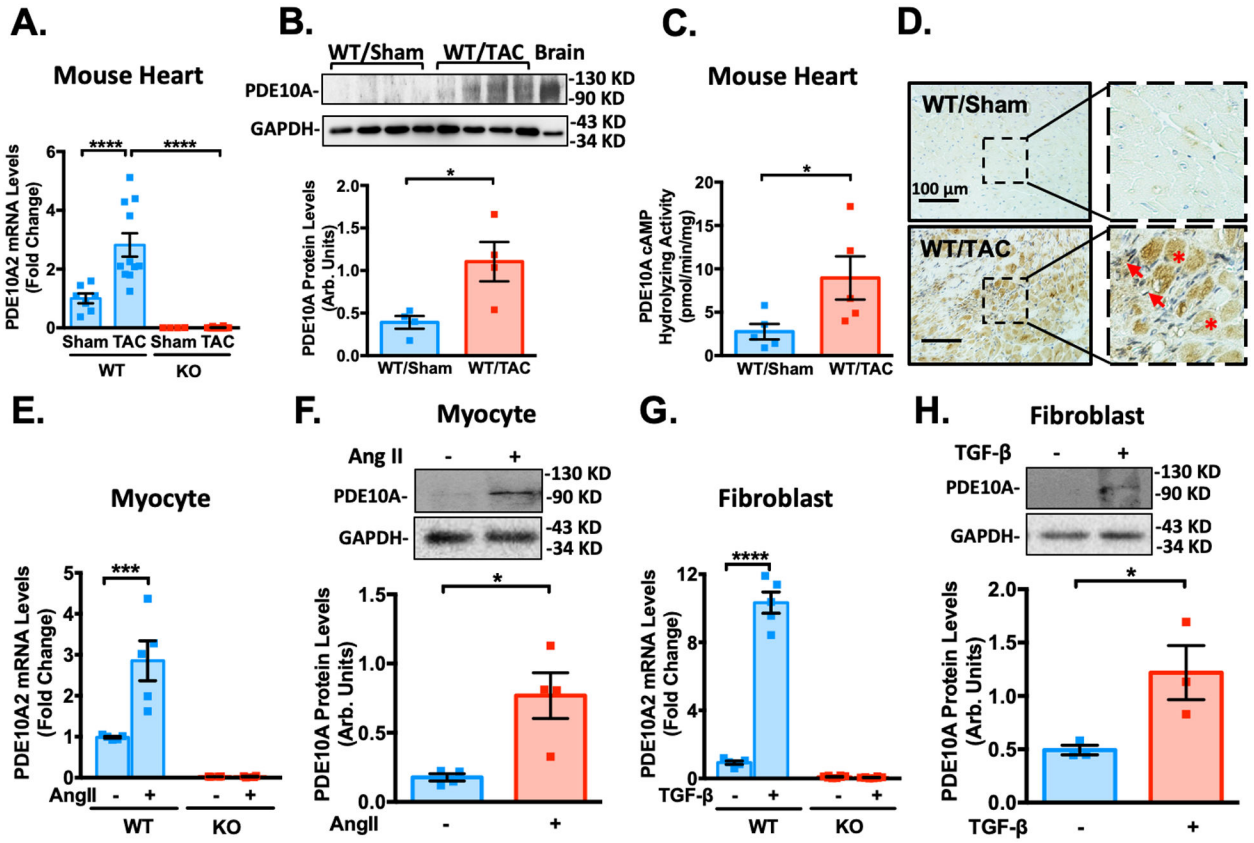

Figure 1: PDE10A expression is upregulated in mouse failing hearts as well as in isolated cardiac myocytes (CMs) and cardiac fibroblasts (CFs).

(A) PDE10A2 mRNA levels assessed by qPCR in mouse heart tissues from mice with 8 weeks of TAC or sham operation, normalized to GAPDH. n=7 for PDE10A-WT/Sham; n=11 for PDE10A-WT/TAC; n=4 for PDE10A-KO/Sham; and n=12 for PDE10A-KO/TAC. (B) PDE10A protein levels measured by western blotting in mouse tissues from mice with 8 weeks of TAC or sham operation, bar graph shows the average of n=4 WT/Sham; n=4 WT/TAC. (C) PDE10A cAMP-hydrolyzing activity in mouse heart tissues from mice with 8 weeks of TAC or sham operation; n=5 for WT/Sham; and n=5 for WT/TAC. (D) Immunohistochemistry staining of PDE10A in myocardium of WT mouse hearts with sham or TAC operation for 8 weeks. Arrows indicate activated CFs. Asterisks indicate CMs. Scale bars: 100 μm. Similar results were obtained from 3 pairs of tissue samples. (E) PDE10A2 mRNA levels assessed by qPCR in mouse adult CMs isolated from PDE10A-WT and -KO mice and stimulated with Ang II (100nM) or vehicle for 72 h, normalized to GAPDH; n=5 replicates from 4 PDE10A-WT mice and n=4 replicates from 4 PDE10A-KO mice. (F) PDE10A protein levels measured by western blotting in CMs isolated from PDE10A-WT mice and stimulated with Ang II (100nM) for 72 h; bar graph shows the average of n=4 replicates from 3 hearts. (G) PDE10A2 mRNA levels assessed by qPCR in CFs isolated from PDE10A-WT and -KO mice and stimulated with TGF-β (10ng/ml) or vehicle for 24 h, normalized to GAPDH; n=5 replicates from 4 PDE10A-WT mice and n=8 replicates from 5 PDE10A-KO mice. (H) PDE10A protein levels measured by western blot in CFs isolated from PDE10A-WT mice and stimulated with TGF-β (10ng/ml) for 24 h; bar graph shows

the average of n=3 replicates from 3 hearts. All data represents the mean ± SEM. Statistics in A, E and G were performed using a two-way ANOVA and Holm-Sidak post-hoc test. Statistics in B-C, F and H were performed using a student t-test. *P < 0.05, ***P < 0.001, ****P < 0.0001.

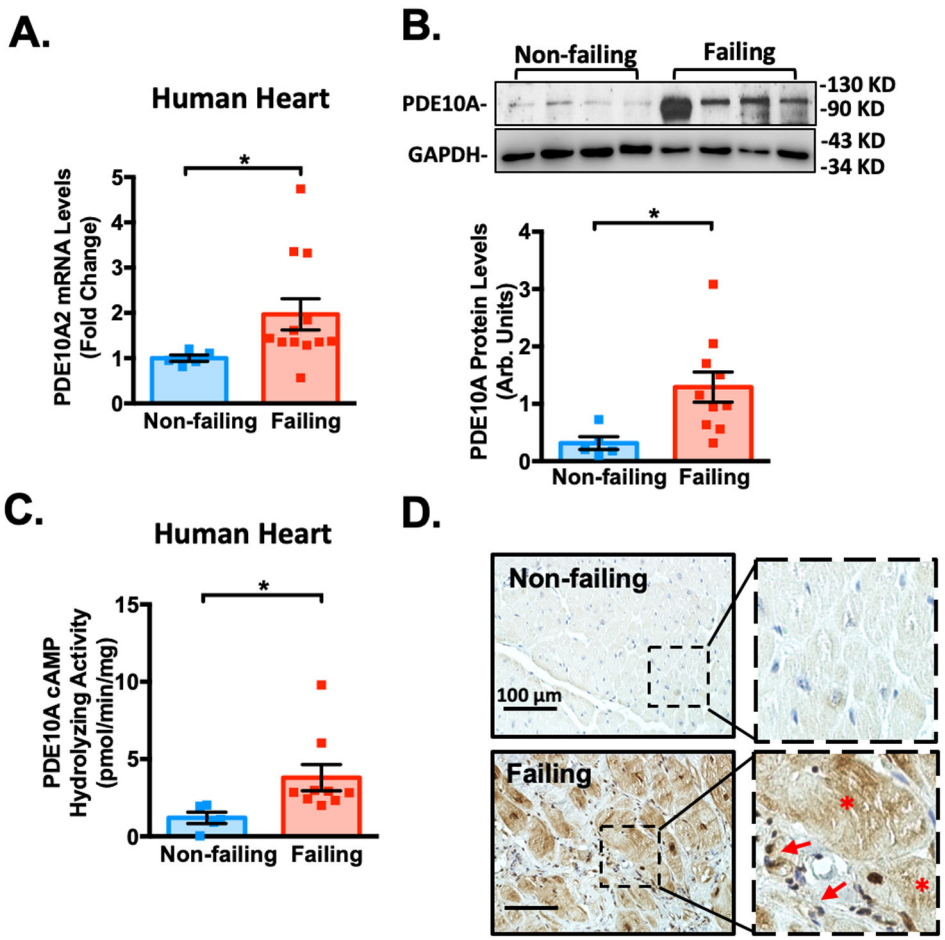

Figure 2: PDE10A expression is upregulated in human failing hearts.

(A) PDE10A2 mRNA levels assessed by qPCR in human non-failing or failing heart tissues, normalized to GAPDH; n=5 for non-failing hearts; n=12 for failing hearts. (B) PDE10A protein levels measured by western blotting in human non-failing or failing heart tissues; bar graph shows the average of n=5 for non-failing hearts and n=10 for failing hearts. (C) PDE10A cAMP-hydrolyzing activity in human non-failing or failing heart tissues; n=5 for non-failing hearts; n=9 for failing hearts. (D) Immuno-histochemistry staining of PDE10A in the human non-failing and failing heart tissues. Arrows indicate activated cardiac fibroblasts (CFs). Asterisks indicate cardiac myocytes (CMs). Scale bars: 100 µm. Similar results were obtained from 3 pairs of tissue samples. Statistics in A-C were performed using a student t-test. *P < 0.05

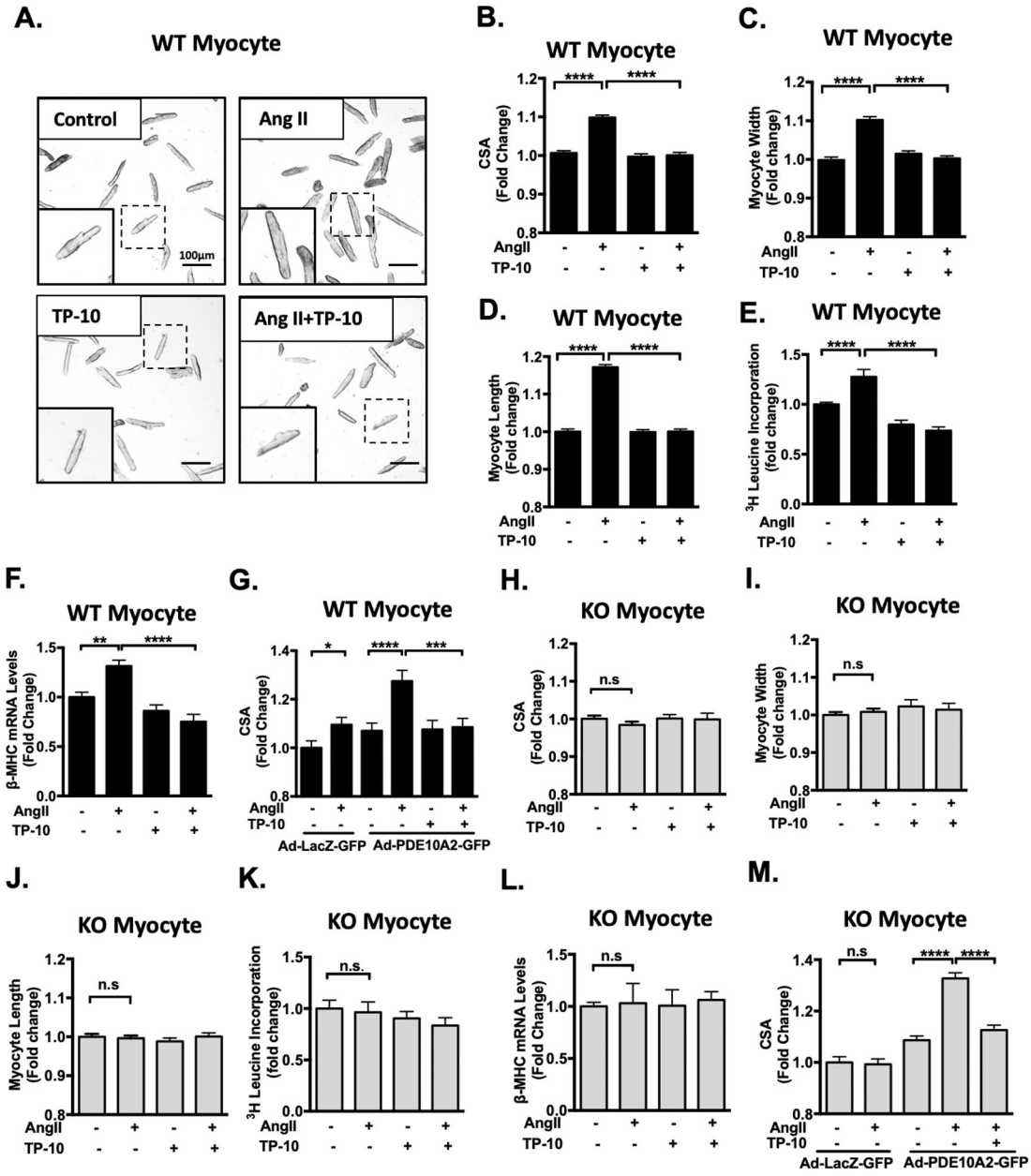

Figure 3: PDE10A inhibition attenuates Ang II-stimulated cardiac myocyte hypertrophy *in vitro*.

(A) Representative images of cardiac myocytes (CMs) isolated from PDE10A-WT mice and pretreated with TP-10 (5 μM) or vehicle, followed by Ang II (100 nM) or vehicle treatment for 72 h. Cells were then fixed and photographed under a microscope. Scale bars: 100 μm. CM cell surface areas (CSAs) (B), width (C) and length (D) were averaged from n > 1500 CMs from 5–7 isolations. (E) [^{3}H]-leucine incorporation in CMs; n = 5–6 replicates from 3 mice. (F) qPCR results showing the mRNA levels of β-MHC, normalized to GAPDH; n= 5–6 replicates from 3 mice. (G) PDE10A-WT CMs were infected with adenovirus expressing LacZ-GFP or PDE10A2-GFP for 24 hours. Cells were then treated with Ang II (100 nM), TP-10 (5 μM) as indicated for 48 hours. (H-M) CMs isolated from PDE10A-KO mice pretreated with TP-10 (5 μM) or vehicle, followed by Ang II (100nM) or vehicle treatment

for 72 h. CSAs (H), width (I) and length (J) were averaged from n > 1500 myocytes from 5–7 isolations. (K) [^{3}H]-leucine incorporation in CMs; n = 5–6 replicates from 3 mice. (L) qPCR results showing the mRNA levels of β-MHC, normalized to GAPDH; n= 5–6 replicates from 3 mice. (M) PDE10A-KO CMs were infected with adenovirus expressing LacZ-GFP or PDE10A2-GFP for 24 hours. Cells were then treated with Ang II (100 nM), TP-10 (5 μM) as indicated for 48 hours. CSAs were averaged from n > 500 CMs from 3 isolations. All data represents the mean ± SEM. Statistics were performed using a two-way ANOVA and Holm-Sidak post-hoc test. *P < 0.05, **P < 0.01, ***P < 0.001, ****P < 0.0001. n.s.: no significant difference.

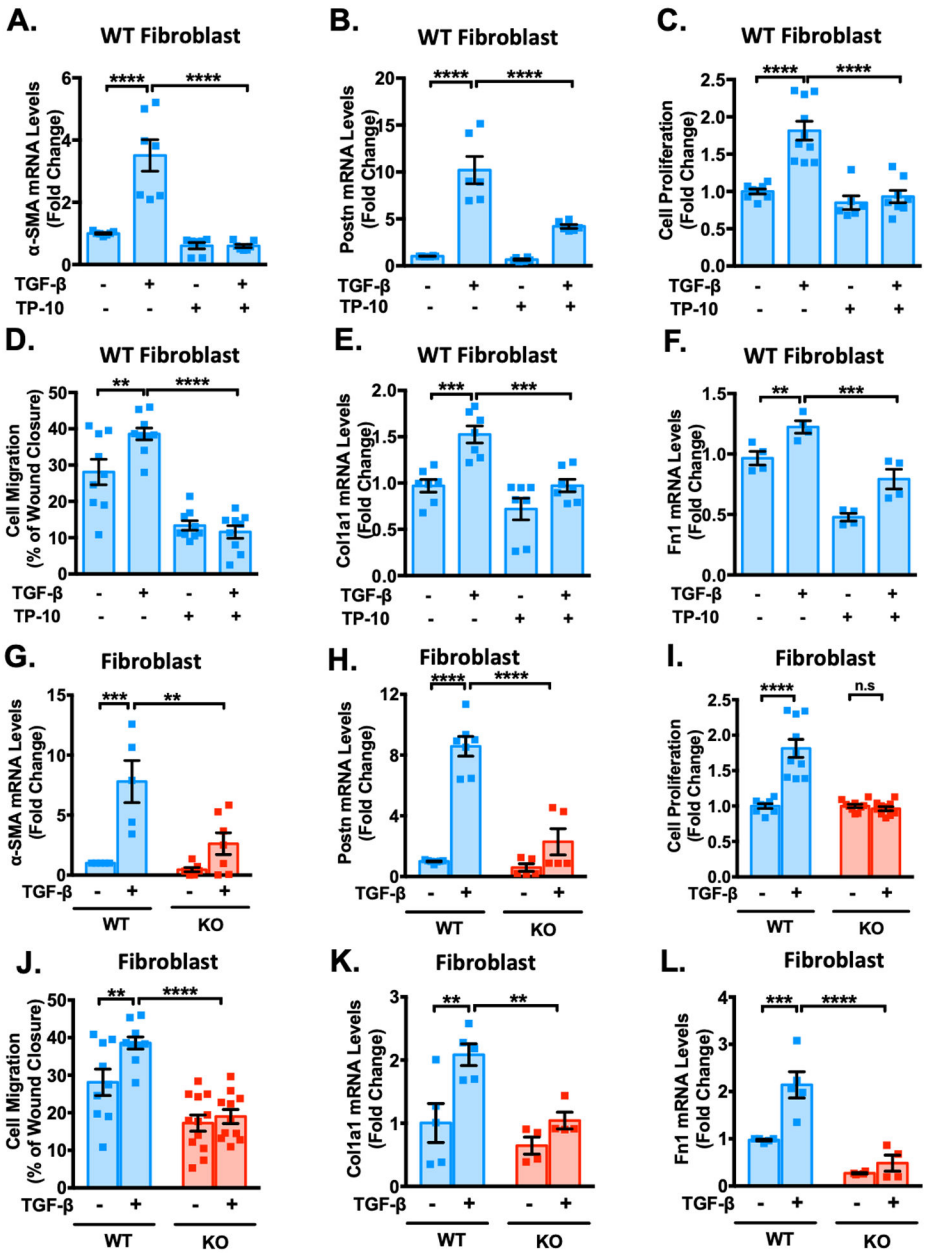

Figure 4: PDE10A inhibition and deficiency attenuate TGF-β-stimulated cardiac fibroblast activation, proliferation, migration and ECM synthesis and *in vitro*.

Cardiac fibroblasts (CFs) isolated from PDE10A-WT or PDE10A-KO mice as indicated, serum starved for 24 h, and pretreated with TP-10 (5 μM) or vehicle, followed by TGF-β (10ng/ml) or vehicle treatment for 24 h or 48 h. mRNA levels of α-SMA (A) and Postn (B) were assessed via qPCR, normalized to GAPDH; n = 4–7 replicates from 3 mice. (C) PDE10A-WT CFs were pretreated with TP-10 (5 μM) or vehicle for 30 min prior to TGF-β (10 ng/ml) for 48 h. Cell proliferation was measured by CCK8 assay; n = 6–10 replicates from 3 mice. (D) After the monolayer formation, PDE10A-WT CFs were serum starved for 24 h and scratches were made in the monolayer. CFs were pretreated with TP-10 (5 μM) or vehicle for 30 min prior to TGF-β (10 ng/ml) for 18 h, and imaged for comparison of wound

closure, n = 9–10 replicates from 4 mice. mRNA levels of Col1a1 (E) and Fn1 (F) were assessed via qPCR, normalized to GAPDH; n = 4–7 replicates from 3 mice. mRNA levels of α-SMA (G), Postn (H) were assessed via qPCR, normalized to GAPDH; n = 5–7 replicates from 3–5 mice. (I) PDE10A-WT or -KO CFs were stimulated with TGF-β (10 ng/ml) for 48 h. Cell proliferation was measured by CCK8 assay; n = 8–10 replicates from 3 mice. (J) After the monolayer formation, PDE10A-WT or -KO CFs were serum starved for 24 h and scratches were made in the monolayer. CFs were stimulated with TGF-β (10 ng/ml) for 18 h, and imaged for comparison of wound closure, n = 9–12 replicates from 4 mice. mRNA levels of Col1a1 (K) and Fn1 (L) were assessed via qPCR, normalized to GAPDH; n = 4–5 replicates from 3–5 mice. All data represents the mean ± SEM. Statistics were performed using a two-way ANOVA and Holm-Sidak post-hoc test. **P < 0.01, ***P < 0.001, ****P < 0.0001. n.s.: no significant difference.

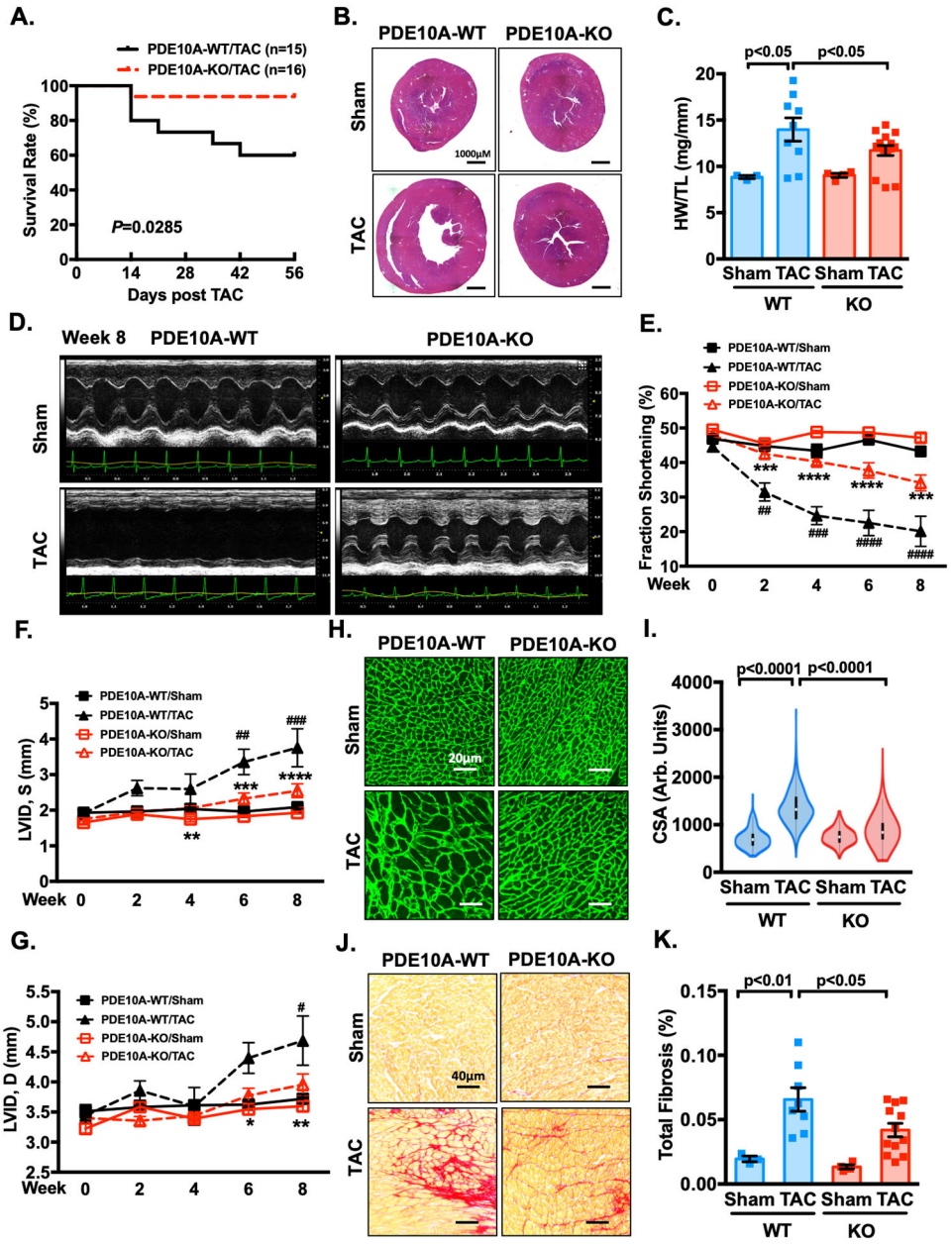

Figure 5: PDE10A deficiency attenuates TAC-induced cardiac remodeling and dysfunction.

Male PDE10A-WT and PDE10A-KO mice at 8–12 week of age were subjected to TAC or sham operation for 8 weeks. (A) The survival curve of PDE10A-WT and PDE10A-KO mice after TAC surgery. P < 0.05, Log-Rank (Mantel-Cox) test. (B) Representative images of hematoxylin and eosin staining in mouse hearts after TAC or sham operation. Scale bars: 1000 μm. (C) Quantification of heart weight/tibia length. (D-G) Cardiac function was monitored via echocardiography at baseline and at 2, 4, 6 and 8 week points after the surgery: (D) representative M-mode echocardiographic images of each study group at 8 week point; (E) progressive percent fraction shortening, (F) left ventricular diameter at systole (LVID,s); and (G) left ventricular diameter at diastole (LVID,d). (H) Representative images of wheat germ agglutinin (WGA)-fluorescein isothiocyanate-staining in mouse

hearts after TAC or sham, showing cardiac myocyte (CM) cross-sectional area (CSA). Scale bars: 20 μm. (I) Quantitative data of CM hypertrophy assessed by CSA; n = 3–12 hearts per group with 300–600 CMs analyzed per heart. (J) Representative images of heart sections stained with picrosirius red. Red staining shows fibrotic areas. Scale bars: 40 μm. (K) Quantification of total fibrosis. All data represents the mean ± SEM. Statistics in C, I and K were performed using a two-way ANOVA and Holm-Sidak post-hoc test. Statistics in E-G were performed using a repeated measures ANOVA and Holm-Sidak post-hoc test. *P < 0.05, **P < 0.01, ***P < 0.001, ****P < 0.0001 PDE10A-KO/TAC vs. PDE10A-WT/TAC; # P < 0.05, ## P < 0.01, ### P < 0.001, #### P < 0.0001 PDE10A-WT/TAC vs. PDE10A-WT/sham. Animal numbers: PDE10A-WT/sham: n = 3 in C, E-G, I and K; PDE10A-WT/TAC: n = 15 in A, n = 9 in C, n = 8 in E-G and K, n = 6 in I; PDE10A-KO/sham: n = 4 in C, E-G, I and K; PDE10A-KO/TAC: n = 16 in A, n = 15 in C, n =12 in E-G, I and K.

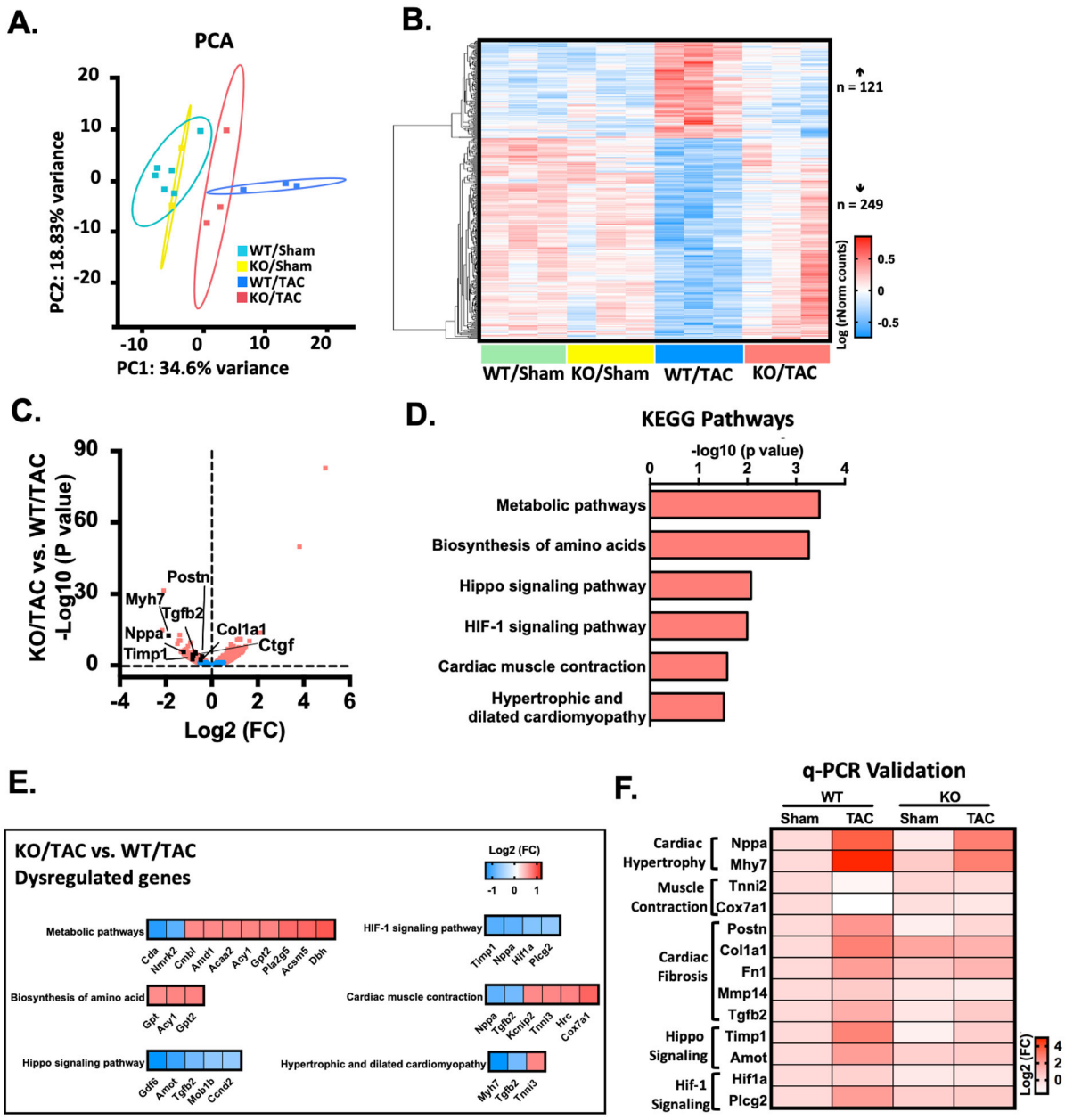

Figure 6: RNA-Seq identifies transcriptome that are dysregulated by PDE10A during heart failure pathogenesis.

(A) Principle component analysis (PCA) reveals the variance in transcriptome distribution in PDE10A-WT and PDE10A-KO hearts at sham and 8 weeks after TAC. Each point represents the projections of individual hearts onto principle component (PC). The majority of genetic variation is addressed by the first (PC1, 34.6%), followed by the second (PC2, 18.83%). (B) Heatmap of genes differentially expressed in PDE10A-WT or PDE10A-KO hearts at 8 weeks after TAC or sham. Each column represents an individual replicate and there are 3 replicates per group. Each row represents an individual gene. The top of heatmap is the cluster of genes that are upregulated in PDE10A-WT/TAC, while the bottom is the cluster of genes downregulated in PDE10A-WT/TAC compared to PDE10A-WT/sham or

PDE10A-KO/sham and reversed in PDE10A-KO/TAC. The color bar represents relative expression of log-transformed, normalized counts with upregulated genes shown in red and downregulated genes in blue. (C) Volcano plot shows magnitude and significance of genes that altered in PDE10A-KO hearts versus PDE10A-WT hearts after TAC. Genes that significantly downregulated (left) and upregulated (right) in PDE10A-KO/TAC versus PDE10A-WT/TAC are plotted in red. Representative known genes involved in pathologic remodeling, such as Myh7, Nppa, Tgfb2, Ctgf, Timp1, Postn and Col1a1, are picked out (black dots) for each volcano plot. (D) Kyoto Encyclopedia of Genes and Genomes (KEGG) pathway analysis of differentially expressed genes in PDE10A-WT and PDE10A-KO after TAC. Signaling pathways are organized in the order of significance as $-\log_{10}$ of P value. P value was corrected by Benjamini & Hochberg multiple test, which < 0.05 was considered significant. (E) Gene list in each KEGG signaling pathway. The color bar represents relative expression of log2-transformed. (F) qPCR validation of cardiac hypertrophic genes Nppa and Myh7, muscle contraction genes Tnni2 and Cox7a1, cardiac fibrotic genes Postn, Col1a1, Fn1, Mmp14 and Tgfb2, hippo signaling related genes Timp1 and Amot, and HIF-1 signaling related genes Hif1a and Plcg2 identified by RNA-seq in the hearts of PDE10A-WT or PDE10A-KO mice after sham or TAC surgery, normalized to GAPDH; n = 3 hearts per group. The color bar represents relative expression of log-transformed.

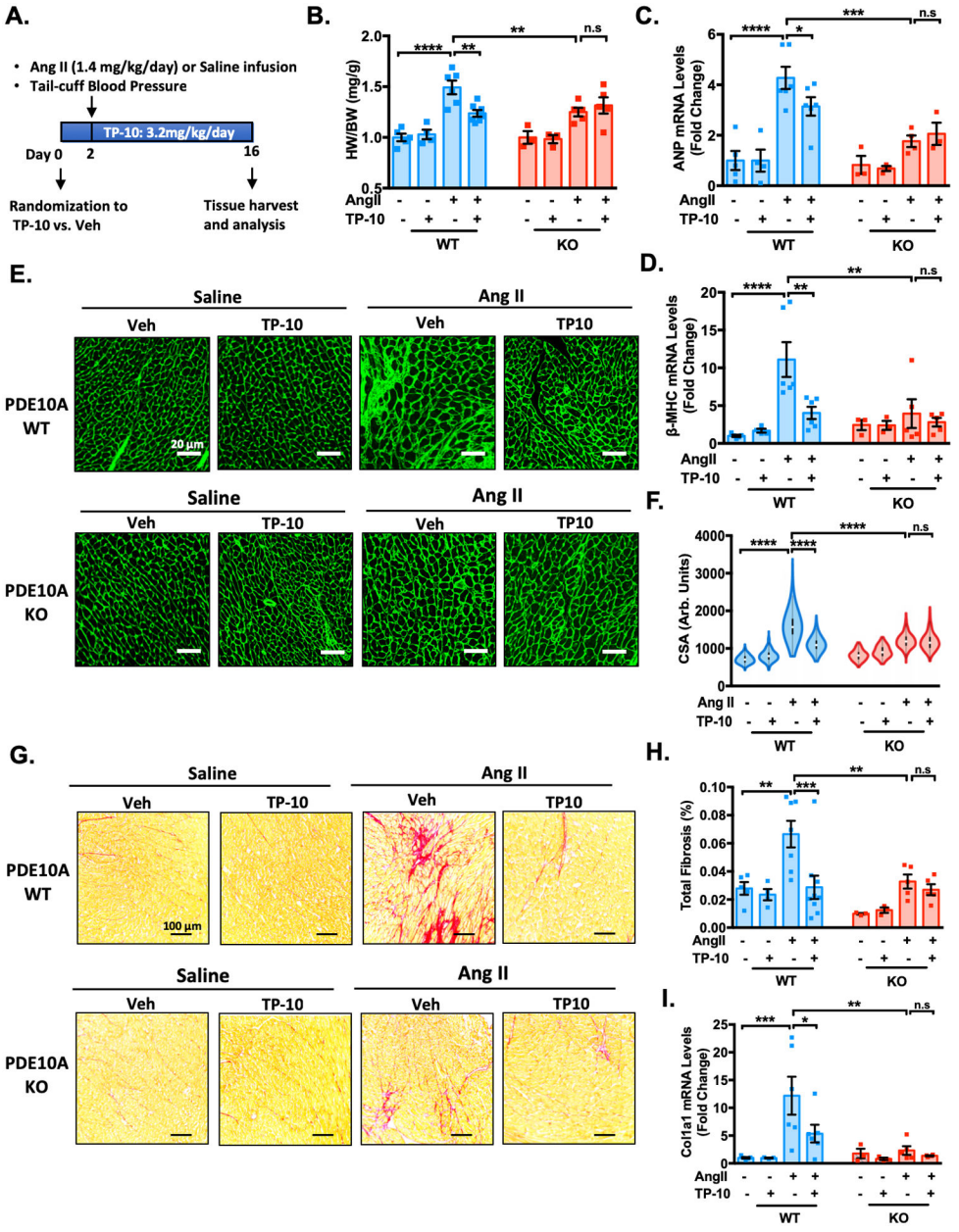

Figure 7: TP-10 attenuates Ang II-induced cardiac remodeling and cardiac fibrosis by specifically inhibiting PDE10A.

PDE10A-WT and PDE10A-KO mice at 8–12 week of age were infused with saline or Ang II (1.4 mg/kg/day) for 2 weeks and administered vehicle or TP-10 (3.2 mg/kg/day) daily via s.c. injection for 16 days (2 days prior and 14 days during Ang II infusion). (A) Experiment timeline. (B) Quantification of heart weight/body weight. (C-D) qPCR analysis of heart failure genes ANP (C) and β-MHC (D) in the hearts of PDE10A-WT or PDE10A-KO mice after saline or Ang II infusion and treatment as indicated, normalized to GAPDH. (E) Representative images of wheat germ agglutinin (WGA)-fluorescein isothiocyanate-staining in mouse hearts showing cardiac myocyte (CM) cross-sectional area (CSA). Scale bars: 20 μm. (F) CM hypertrophy was quantified by assessing CSA from WGA staining; n = 3–9

hearts per group with 300–500 cardiac myocytes measured per heart. (G) Representative images of heart sections stained with picrosirius red. Red staining shows fibrotic areas. Scale bars: 100 μm. (H) Quantification of total fibrosis. (I) qPCR analysis of fibrotic genes Col1a1 in the hearts of PDE10A-WT or PDE10A-KO mice after saline or Ang II infusion and treatment as indicated, normalized to GAPDH. All data represents the mean ± SEM. Statistics were performed using a two-way ANOVA and Holm-Sidak post-hoc test. *P < 0.05, **P < 0.01, ***P < 0.001, ****P < 0.0001. n.s.: no significant difference. Animal numbers: PDE10A-WT/saline infusion/vehicle: n = 5 in B-D, F and H-I; PDE10A-WT/saline infusion/TP-10: n = 4 in B-D, F and H-I; PDE10A-WT/Ang II infusion/vehicle: n = 6 in B-D and I, n = 7 in F-H; PDE10A-WT/Ang II infusion/TP-10: n = 7 in B, n = 6 in C-D and I, and n = 9 in F-H; PDE10A-KO/saline infusion/vehicle: n = 3 in B-D, F and H-I; PDE10A-KO/saline infusion/TP-10: n = 3 in B-D, F and H-I; PDE10A-KO/Ang II infusion/vehicle: n = 5 in B, D, F and H-I, and n = 4 in C; PDE10A-KO/Ang II infusion/TP-10: n = 5 in B, D, F and H, n = 3 in C, and n = 4 in I.

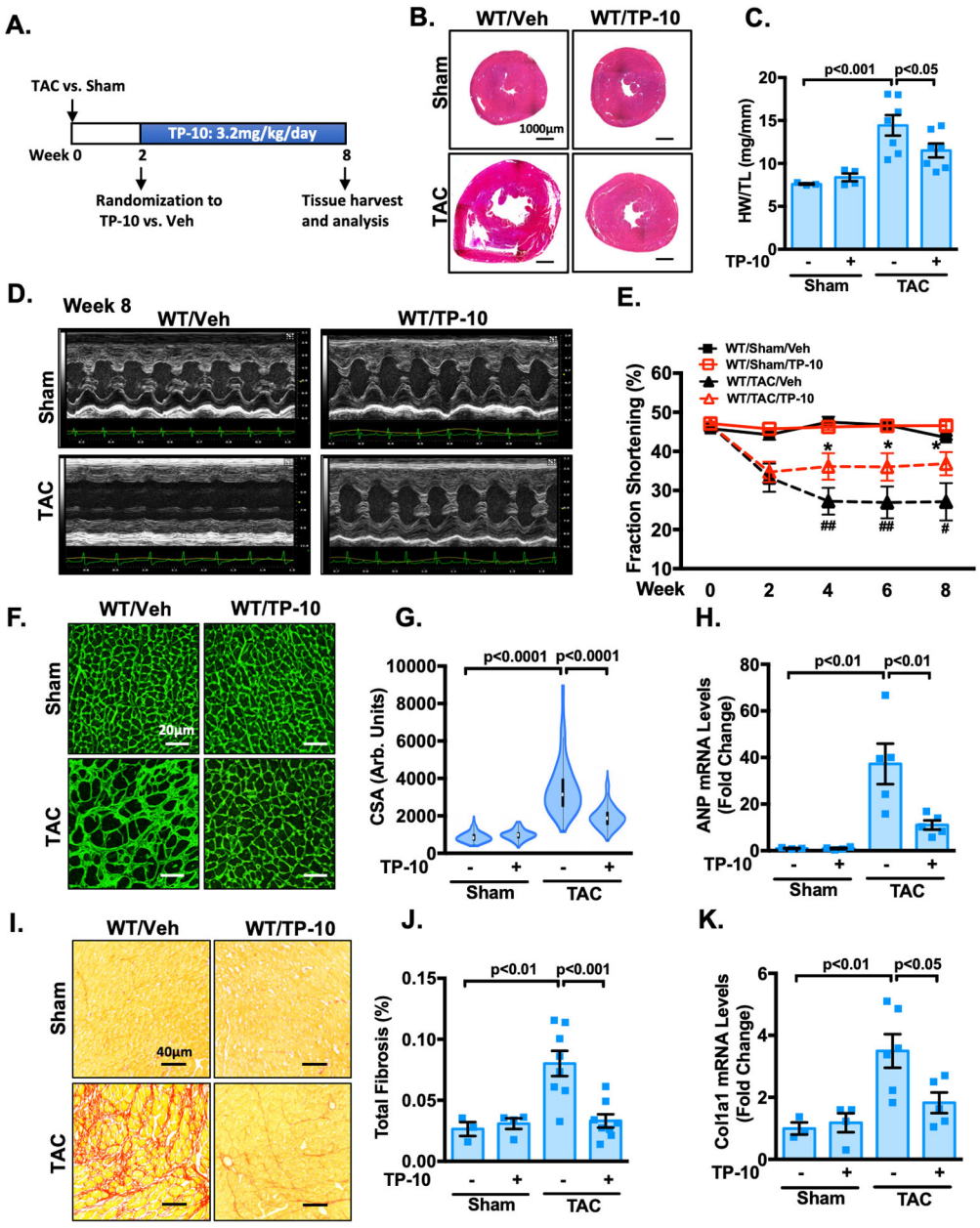

Figure 8: TP-10 intervenes the progression of pre-stimulated cardiac remodeling and dysfunction.

Male WT mice at 8–12 week of age were subjected to TAC or sham operation for 8 weeks. Mice were then randomized to receive either TP-10 (3.2mg/kg/day) or vehicle treatment 2 weeks after sham or TAC and the drug treatment was continued for 6 weeks. (A) Experiment timeline. (B) Representative images of hematoxylin and eosin staining in mouse hearts after TAC or sham operation with vehicle or TP-10 treatment as indicated. Scale bars: 1000 μm. (C) Quantification of heart weight/tibia length. (D-E) Cardiac function was monitored via echocardiography at baseline and at 2, 4, 6 and 8 week points after the surgery. (D) representative M-mode echocardiographic images of each study group. (E) progressive percent fraction shortening. (F) Representative images of wheat germ agglutinin (WGA)-

fluorescein isothiocyanate-staining in mouse, showing cardiac myocyte (CM) cross-sectional area (CSA). Scale bars: 20 μm. (G) Quantitative data of CM hypertrophy assessed by CSA; n = 3–6 hearts per group with 150–300 CMs analyzed per heart. (H) qPCR analysis of heart failure genes ANP, normalized to GAPDH. (I) Representative images of heart sections stained with picrosirius red. Red staining shows fibrotic areas. Scale bars: 40 μm. (J) Quantification of total fibrosis. (K) qPCR analysis of fibrotic genes Col1a1, normalized to GAPDH. All data represents the mean ± SEM. Statistics in C, G-H and J-K were performed using a two-way ANOVA and Holm-Sidak post-hoc test. Statistics in E was performed using a repeated measures ANOVA and Holm-Sidak post-hoc test. *P < 0.05 WT/TAC/TP-10 vs. WT/TAC/vehicle; # P < 0.05, ## P < 0.01 WT/TAC/vehicle vs. WT/sham/vehicle. Animal numbers: WT/sham/vehicle: n = 3 in C, E, G-H and J-K; WT/sham/TP-10: n = 4 in C, E, G-H and J-K; WT/TAC/vehicle: n = 7 in C, E, G, n = 5 in H and K, n = 8 in J; WT/TAC/TP-10: n = 7 in C, n = 8 in E, G and J, n = 5 in H and K.